Biochemical and Biophysical Research Communications 425 (2012) 769–774

Contents lists available at SciVerse ScienceDirect

Biochemical and Biophysical Research Communications

journal homepage: www.elsevier.com/locate/ybbrc

# Bacteria-mediated *in vivo* delivery of quantum dots into solid tumor

Ying Liu [a], Mei Zhou [b], Dan Luo [a], Lijun Wang [a], Yuankai Hong [a], Yepeng Yang [b], Yinlin Sha [a,c,*]

[a] Single-molecule and Nanobiology Lab., Dept. of Biophysics, School of Basic Medical Sciences, Peking University, No. 38 Xue Yuan Road, Beijing 100091, China
[b] Dept. of Radiation Medicine, School of Basic Medical Sciences, Peking University, No. 38 Xue Yuan Road, Beijing 100091, China
[c] Biomed-X Center, Peking University, Peking University, No. 38 Xue Yuan Road, Beijing 100091, China

ARTICLE INFO

*Article history:*
Received 25 July 2012
Available online 4 August 2012

*Keywords:*
Quantum dots
*Bifidobacterium bifidum*
Electroporation
*In vivo* imaging

ABSTRACT

Semiconductor nanocrystals, so-called quantum dots (QDs), promise potential application in bioimaging and diagnosis *in vitro* and *in vivo* owing to their high-quality photoluminescence and excellent photostability as well as size-tunable spectra. Here, we describe a biocompatible, comparatively safe bacteria-based system that can deliver QDs specifically into solid tumor of living animals. In our strategy, anaerobic bacterium *Bifidobacterium bifidum* (*B. bifidum*) that colonizes selectively in hypoxic regions of animal body was successfully used as a vehicle to load with QDs and transported into the deep tissue of solid tumors. The internalization of lipid-encapsuled QDs into *B. bifidum* was conveniently carried by electroporation. To improve the efficacy and specificity of tumor targeting, the QDs-carrying bacterium surface was further conjugated with folic acids (FAs) that can bind to the folic acid receptor overexpressed tumor cells. This new approach opens a pathway for delivering different types of functional cargos such as nanoparticles and drugs into solid tumor of live animals for imaging, diagnosis and therapy.



## 1. Introduction

Semiconductor nanocrystals, so-called quantum dots (QDs), have attracted widespread interests in fields ranging from chemistry [1], material science [2], device engineering [3] to biological applications [4,5], owing to their high-quality photoluminescence and excellent photostability as well as size-tunable spectra [6–8]. In comparison with organic fluorophores whose observation time are limited by photobleaching, the excellent fluorescent intensity and long-term stability of QDs give them the potential to become superb fluorescent markers for *in vivo* imaging. When being applied *in vivo* biological imaging, QDs are usually covalently linked to biorecognition molecules such as antibodies [9,10] and peptides [11,12] as fluorescent probes. Gao et al. designed antibody-binding, PEG-encapsulated QDs to target human prostate tumor *in vivo* open a new way for QDs *in vivo* tumor imaging [9]. However, there are a series of issues in connection with biorecognition molecules and PEG on the surface of QDs that cannot be ignored, such as an increase in molecular weight of the bioconjugated QDs which may lead to a loss of solubility in body fluid, which in turn will lead to a low targeting efficiency [13]. Meanwhile, the clearance of the reticuloendothelial system (RES) of bioconjugated QDs is also a tremendous obstacle that is hard to get through. QDs will be attacked and cleared when they enter the blood vessels [14]. In order to have an effective imaging *in vivo* using QDs, it is crucial to design a delivery system which has the following properties: a high targeting efficacy of the tumor tissue and an excellent *in vivo* biocompatibility.

Probiotic bacteria such as *Bifidobacterium bifidum* can genetically localize and distribute in tumor tissues of mammalian bodies and are nonpathogenic and almost nontoxic to the host [15–17]. Taking advantages of the intrinsic properties of probiotic bacteria, several groups that transferred genes to solid tumors are achieved [18–21]. In 1980, Kimura first reported that *B. bifidum* can selectively localize and proliferate in tumor hypoxic zone via systemic intravenous method. After 48–96 h of injection, *B. bifidum* existed only in tumor tissue but none in blood, bone marrow, muscle, liver, spleen, kidney and lung. In tumor tissue, up to $10^6$ bacterial clones could be detected. This feature was attributed to the tumor tissue hypoxic microenvironment which was suitable for the localization of *B. bifidum* [21]. Here, we used *B. bifidum* as a vehicle to load with QDs and transport into the deep tissue of solid tumors for the following reasons: First, as a typical probiotic bacteria existing in many kinds of mammalian bodies including human beings, *B. bifidum* has been proven to be safe, without pathogenic or immunogenic side effects. Second, as a type of anaerobic bacteria, *B. bifidum* only colonizes in hypoxic tissues and this gives them the potential to settle in the deep tissues of the solid tumors, rather than normal organs and tissues. Third, the peptidoglycan-rich surface of bacteria allows further chemical modifications, such as

* Corresponding author at: Single-molecule and Nanobiology Lab., Dept. of Biophysics, School of Basic Medical Sciences, Peking University, No. 38 Xue Yuan Road, Beijing 100091, China. Fax: +86 10 82801278.
*E-mail addresses:* yangyepeng@bjmu.edu.cn (Y. Yang), shyl@hsc.pku.edu.cn (Y. Sha).

0006-291X/$ - see front matter © 2012 Elsevier Inc. All rights reserved.
http://dx.doi.org/10.1016/j.bbrc.2012.07.150

ligation of targeting molecules, to improve the specificity and efficacy of QDs delivery. Fourth, the micron-scaled *B. bifidum* has enough space inside for the nano-sized QDs to embed.

In this paper, we used the anaerobic *B. bifidum*, a typical probiotic bacteria existing in many kinds of mammalian bodies including human beings, as a vehicle to deliver QDs into the solid tumor of living mice via systemic intravenous method. We further modified the bacteria by joining the FAs to the bacteria surface, in order to improve the targeting efficacy of the bacteria to tumor tissue. Combining the advantages of their intrinsic biocompatibility and easy preparation, the chemically modified *B. bifidum* could be used as a versatile vehicle to efficiently deliver probes and therapeutic reagents for cancer diagnostics and therapy.

## 2. Materials and methods

### 2.1. Chemicals

All chemicals were used directly without further purification. Cadmium oxide (CdO, 99.0%, Shuanghuan Weiye Reagent Co.), sulfur powder (S, 99.5%, Sinopharm Chemical Reagent Co.), selenium powder (Se, 99.95%, Meixing Chemical Reagent Co.), oleic acid (OA, 97%, Kermel Chemical Reagent Co.), tri-*n*-octylphosphine oxide (TOPO, 99%, Fluka), tri-*n*-octylamine (TOA, 97%, Yuanyue Chemical Co.), folic acid (FAs, >96%, Acros), 3-(4,5-dimethylthiazol-2-yl)-2,5-diphenyltetrazolium bromide (MTT, 98%, Amresco). Dimethyl sulfoxide (DMSO, 99%) and palmitoyloleoylphosphatidylcholine (POPC) were purchased from Sigma–Aldrich. Chloroform and ethanol were purchased from Beijing Chemical Co. Ultrapure water (18.2 MΩ $cm^{-1}$) was used in the experiments.

### 2.2. Instruments

Absorption spectra were acquired with a TU-1901 UV–Vis spectrophotometer (Beijing PuXiTongYong Co.). Photoluminescence (PL) spectra were recorded on an F-4500 fluorescence spectrophotometer (Hitachi). Differential interference contrast (DIC) and fluorescent imaging were performed on an IX 71 inverted microscope with a 60× oil immersion objective (NA 1.45, Olympus), equipped with an EMCCD (iXon DV-887, Andor). The digital images were collected and analyzed by using IPLab software (BD Biosciences Bioimaging).

#### 2.2.1. CdSeS QDs synthesis

Ternary CdSeS QDs were prepared by the reported method [22]. Typically, CdO (256.8 mg), oleic acid (OA, 2.5 mL), and tri-*n*-octylamine (TOA, 20 mL) were mixed in a three-necked flask, and heated to 300 °C under an argon atmosphere to get a clear solution. A stock solution of Se (9.5 mg, 0.12 mmol) and S (192.0 mg, 6.0 mmol) in TOPO (1.0 mL) was swiftly injected into the hot solution, and the reaction was allowed to proceed at 280 °C for 1 min. CdSeS QDs were obtained with ethanol sedimentation and repeatedly washed with ethanol. The prepared CdSeS QDs displayed a fluorescent emission ($\lambda_{em}$, max 576 nm) with the full-width at the half-maximum (FWHM) near 30 nm.

#### 2.2.2. Preparation of $QD_{576}$–POPC micelles

The prepared $QD_{576}$ (1.0 mg) was first dissolved in POPC solution of chloroform (0.5 mL, 1.0 mg $mL^{-1}$). Then the solvent was removed at 45 °C with a rotary evaporator, and ultrapure water (1.0 mL) was added. The mixed solution was oscillated at 60 °C using an ultrasonic oscillator to obtain an optically clear solution of $QD_{576}$–POPC micelles.

#### 2.2.3. B. bifidum culture

*Bifidobacterium bifidum* (CGMCC 1.2212) was anaerobically cultured at 37 °C to early-log phase in broth. The culture was grown for 5 h at 37 °C with an incubator shaker at 250 rpm until the optical density ($\lambda$ = 600 nm) reached 0.3–0.4. The *B. bifidum* was harvested by chilling the flasks briefly on ice and centrifuging at 2000*g* for 20 min at 4 °C.

#### 2.2.4. Electroporation

The experiments were carried out on a gene pulser apparatus (Scientz Co.) with the capacitance of 25 μF. *B. bifidum* (150 μL, $1.5 \times 10^5$ $mL^{-1}$) and $QD_{576}$–POPC solution (150 μL, 0.01 mg $mL^{-1}$) were mixed in a cold tube and then transferred into a cuvette (pathlength, 0.2 cm). The electroporation was performed under an optimum experimental condition (1.5 kV, 300 Ω, 60 min). After a post-pulse incubation (shaking at 150 rpm for 1 h at 37 °C), the treated bacteria were washed with PBS in a centrifuge (phosphate buffered saline, pH 7.4) to remove the free $QD_{576}$–POPC micelles.

#### 2.2.5. FAs connected to the bacterial surface

Briefly, *B. bifidum* or QDs-*B. bifidum* (2 mL, $1 \times 10^5$ $mL^{-1}$) was mixed with the FAs solution dissolved in PBS (1.0 mL, 10 mg $mL^{-1}$, pH 7.6) in a 10-mL round-bottomed flask. Then EDC (10.0 mg, 50 μmol) and sulfo-NHS (22.0 mg, 100 μmol) were added. In order to maintain an anaerobic condition, oxygen was driven out by argon flow in the experiments. The reactions proceeded for about 4 h at 37 °C, and the un-reactants were fully removed by quickly centrifuging at 10,000*g* for 30 s at room temperature for three times. The obtained FAs-modified bacteria were redispersed in appropriate amount of PBS (pH 7.4).

#### 2.2.6. Solid tumor tissue imaging

The animal experiments were performed in accordance with the guidelines of the National Institute of Health of the USA. The solid tumor-bearing mice model was established by inoculation of the cultured Lewis lung cancer cells dispersed in PBS (pH 7.4; 0.2 mL, and $1 \times 10^6$ $mL^{-1}$) into the left thigh muscle of mice (6–8 week age, male C57BL/6N mice with weight of about 20 ± 1 g). When the tumor grew to about 10 ± 0.5 mm in diameter, QDs-*B. bifidum* or QDs-*B. bifidum*–FAs dispersed in PBS (pH 7.4; 0.2 mL, and $1 \times 10^5$ $mL^{-1}$) were injected into the tail vein. The mice were

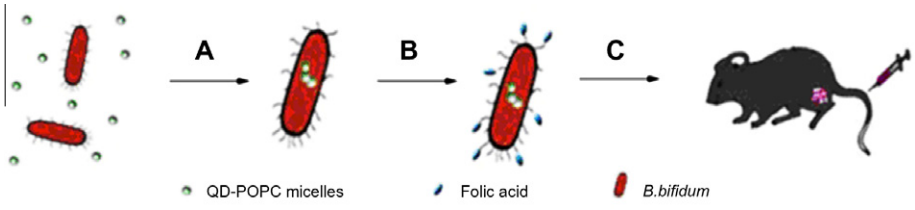


**Fig. 1.** Schematic illustration of QDs delivery. (A) Electroporation; (B) *B. bifidum* surface modification with FAs; (C) intravenous administration.

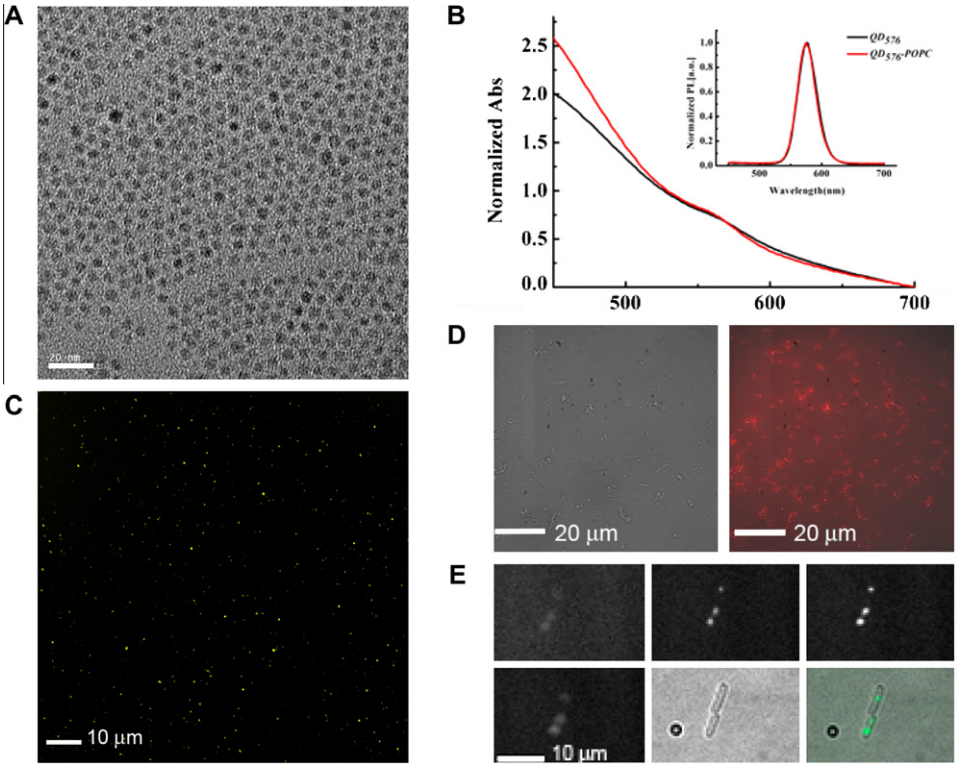


**Fig. 2.** (A) Electron microscopy image of $QD_{576}$; (B) normalized absorption and fluorescence spectra of $QD_{576}$ (black lines) and $QD_{576}$–POPC micelles (red lines); (C) fluorescent image of $QD_{576}$–POPC micelles; (D) differential interference contrast (DIC) and fluorescent images of QDs-*B. bifidum*; (E) confocal microscopy fluorescent images, DIC image (bottom middle) and overlapped image (bottom right) of QDs-*B. bifidum*.

sacrificed on the 1st, 2nd, 3rd, 4th and 5th days, and the tumor tissue slices were fixed with 10% formalin for 24 h and embedded with paraffin. The slices were about 4 μm in thickness for fluorescent imaging.

#### 2.2.7. Whole animal imaging

The whole mouse fluorescent imaging was performed on an EXPLOREMORE system (ColdSpring Co.), equipped with a 300-W high-pressure mercury lamp, an EMCCD (iXon DV-887, Andor), and a tunable liquid crystal filter (VariSpec, CRI Inc.). The mice were anaesthetized with diethyl ether before the fluorescent imaging. The autofluorescent signals were removed using the unmixing function of Image J software (Ver. 1.34s).

## 3. Results and discussion

### 3.1. CdSeS QDs synthesis and lipid encapsulation

Ternary CdSeS QDs passivated by hydrophobic ligands TOPO and OA were synthesized according to the previous reports [22–24]. The QDs PL could be precisely tuned by conveniently controlling the relative molar ratio of chemical precursors in the experiments (Section 2). As shown in Fig. 2, the prepared CdSeS $QD_{576}$ ($\lambda_{em}$ = 576 nm) exhibited a broad absorption cross-section, a sharp and symmetrical band gap emission (FWHM < 30 nm) as well as an uniform sized distribution (diameter = 4.4 ± 0.4 nm ($n$ = 100)).

It is known that liposome is an efficient carrier of plasmid, RNAs and drugs [25]. In order to transfer QDs into the *B. bifidum*, the CdSeS QDs were encapsulated by POPC. As shown in Fig. 2, the prepared POPC encapsulated CdSeS $QD_{576}$ micelles ($QD_{576}$–POPC) retained the optical quality of the uncoated CdSeS $QD_{576}$ and were homogeneously dispersed in aqueous solutions.

### 3.2. Electroporation

Electroporation is a traditional method to increase permeability of the cell plasma membrane by an externally applied electrical field, and has been widely used as a way of introducing exogenous substance into cells. Because *B. bifidum* has not only a cytoplasmic membrane as mammalian cells, but also a rigid wall, we optimized the electroporation conditions (voltage, resistance and post-pulse incubation time) to improve the transferring efficacy (see Supporting information, Figs. S1–3). The optimal electroporation parameter was voltage = 1.5 kV, resistance = 300 Ω, post-pulse incubation time = 60 min. Fig. 2d showed the $QD_{576}$–POPC loaded *B. bifidum* (QDs-*B. bifidum*) under the optimum experimental condition (1.5 kV, 300 Ω, 60 min), and over 66.8% of bacteria had been loaded with $QD_{576}$–POPC micelles. Confocal imaging further confirmed that $QD_{576}$–POPC micelles had been transferred into *B. bifidum* (Fig. 2e). Cellular viability test showed that QDs-*B. bifidum* was a kind of high dynamic probe (Fig. S2). Moreover, the fluorescent intensity of QDs-*B. bifidum* was stable under the *B. bifidum* culture conditions and was detectable even after more than 50 days. As we have postulated, it could be associated with the protection of the POPC layer and the cellular shell, as well as the hypoxic environment, in which the decomposition of QDs was depressed.

### 3.3. In vivo tumor targeting

The *in vivo* QDs delivery was performed in a tumor-bearing mice model that was established by inoculation of Lewis lung cancer cells under skin of mice (Male C57BL/6N, Peking University Health Science Center). Briefly, when the solid tumor reached about 10 ± 0.5 mm in diameter, about $2 \times 10^4$ bacilli/mouse QDs-*B. bifidum* dispersed in PBS (pH 7.4; 0.2 mL, $1 \times 10^5$ $mL^{-1}$)

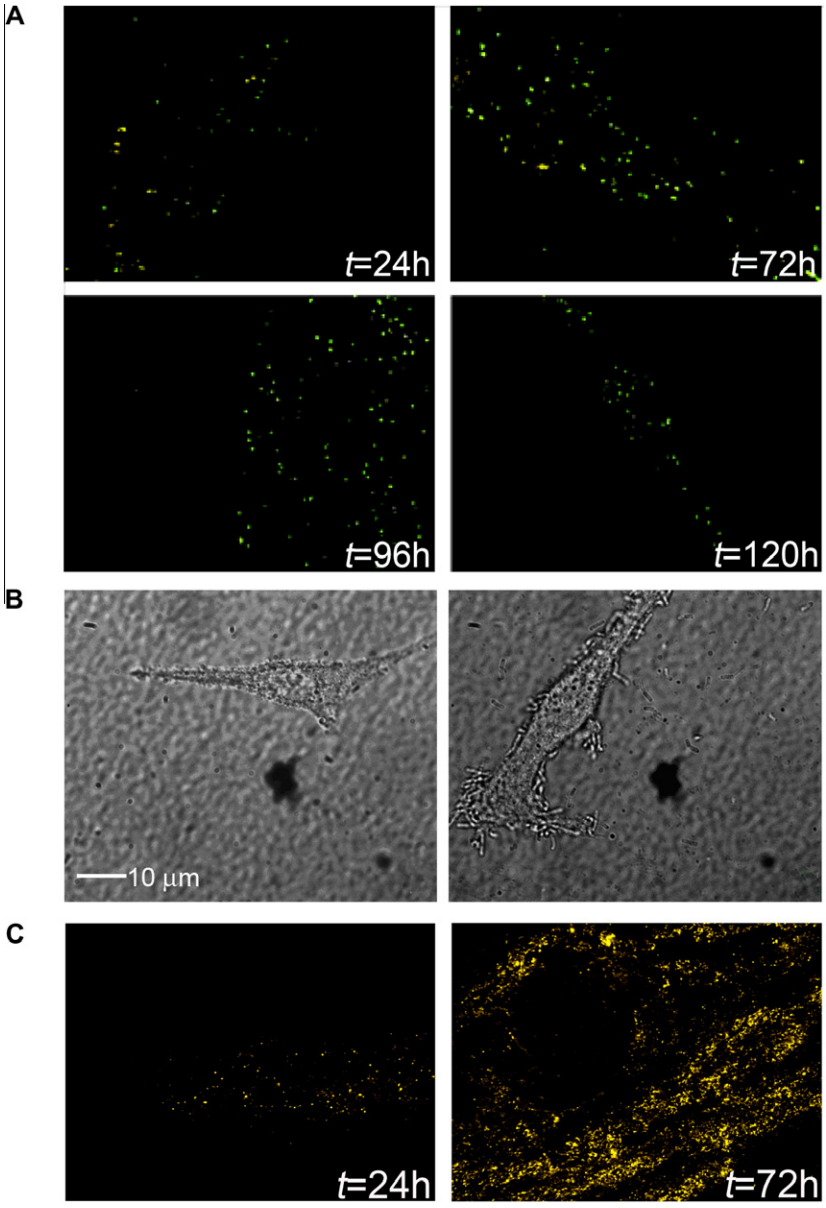


**Fig. 3.** Fluorescent images of solid tumor tissue slices at different time after intravenous injection of (A) QDs-*B. bifidum* and (C) QDs-*B. bifidum*–FAs, respectively; (B) DIC images of Lewis lung cancer cells after incubation with QDs-*B. bifidum* (left) and QDs-*B. bifidum*–FAs (right), respectively.

were injected into the tail vein (Fig. 1). Fig. 3a showed the representative fluorescent images of the solid tumor slices at different time after the QDs-*B. bifidum* administration. The fluorescent signals of QDs were clearly observed after 24 h of administration, and the QDs distribution reached maximal between 72 and 96 h and then gradually attenuated. These results indicated that QDs-*B. bifidum* could reach the deep tissue of solid tumors through bloodstream delivery. This could be associated with the permeability of dysfunctional vasculature of solid tumors and the anaerobic instincts of *B. bifidum*. It is known that the solid tumor growth generally comes with a rapid formation of new blood vessels for supplying oxygen and nutrients. This abnormal vasculature network is generally irregular in structure, with pores in the vessels which favor substances to permeate into the tumor tissue. Hobbs et al. analyzed the functional limits of transvascular transport. They found that the vascular pore cutoff size was between 1.2 and 2 μm [26]. In our studies, *B. bifidum* is approximately 1–2 μm in length and 0.2–0.5 μm in diameter. Therefore, *B. bifidum* could pass through the tumor vasculature freely into the solid tumor.

In another aspect, the abnormal growth of tumor vasculature will cause a hypoxic region formed in the deep sites of tumors, in which the average of partial oxygen pressure can be even less than 2.5 mm Hg [27]. Together with the abnormal vasculature, the hypoxic microenvironment favored QDs-*B. bifidum* to settle and accumulate in solid tumors. It is interesting to note that, in contrast to the reported PEG chemistry-based strategy [28], the circulation half-life of QDs-*B. bifidum* in bloodstream was much longer, and the fluorescent signals could be detected even after 120 h of administration (Fig. 3a). We are of the view that this could be due to the intrinsic biocompatibility of the *B. bifidum* and the high photostability of the encapsulated QDs.

### 3.4. FAs connected to the bacterial surface

Like most of cancer cells, the Lewis lung cancer cells possess overexpressed folic acid receptors on their surface. Thus we modified the QDs-*B. bifidum* with FAs to enhance its binding potential to cancer cells. To avoid possible chemical damage to the bacteria,

the *B. bifidum*–FAs conjugation was conducted in aqueous solution using mild EDC/sulfo-NHS in which the FAs molecules were conjugated onto the peptidoglycan-rich surface of *B. bifidum* via carbonyl amide bonding. By counting bacteria clones, we evaluated the cellular viability of FAs-modified *B. bifidum*. As compared with the normal *B. bifidum*, FAs-modified *B. bifidum* displayed a similar growth curve (Fig. S4), indicating the FAs modification did not affect the viability of *B. bifidum*. Fig. 3b revealed that the FAs-modified QDs-*B. bifidum* (QDs-*B. bifidum*–FAs) had a strong potential to adhere around Lewis lung cancer cells, while *B. bifidum* alone did not. It indicated that the FAs-modification could confer *B. bifidum* with high affinity to tumor cells. The FAs modification induced enhancement of targeting efficacy was demonstrated under *in vivo* conditions. Fig. 3 showed the tissue slices of solid tumors at different time after QDs-*B. bifidum*–FAs and QDs-*B. bifidum* administration via the tail vein of the mice. In comparison with QDs-*B. bifidum*, the fluorescent signals of QDs-*B. bifidum*–FAs distributed in the solid tumor were significantly enhanced under the same condition (Fig. S5).

### 3.5. Live animal imaging

Fig. 4 showed the typical whole-animal fluorescent images of the tumor-bearing mice after the QDs-*B. bifidum*, QDs-*B. bifidum*–FAs and $QD_{576}$–POPC (as control) administration, respectively. It was found that, for both QDs-*B. bifidum* and QDs-*B. bifidum*–FAs administration, the solid tumor profiles were clearly observed. In comparison with QDs-*B. bifidum*–FAs administration, we noted that some fluorescent signals were also observed in the breast part of mice for QDs-*B. bifidum* administration. The result showed that the nonspecific delivery was significantly decreased after FAs modification on *B. bifidum* surfaces. Together with *ex vivo* results (Fig. 3), these data strongly supported that the FAs-modified *B. bifidum* could be used as an efficient vehicle to deliver QDs into the solid tumor of living mice.

It is known that the hypoxic region of solid tumors was a barrier impacting the effectiveness of both radiation therapy and chemotherapy [29,30]. The *B. bifidum*-mediated QDs delivery under *in vivo* conditions opens a possible way to deliver therapeutic agents, such as chemical drugs, radiation elements and photo-therapeutic chemicals into the deep tissue of the solid tumor for enhancing therapy efficacy. The enhancement of the specificity and efficacy of QDs delivery after the surface modification of *B. bifidum* with FAs implied that this strategy could be used for early detection of cancer.

In summary, we have developed a new approach to deliver QDs into the deep tissue of solid tumors in living mice by using the probiotic *B. bifidum* as a vehicle, and the targeting efficacy was further

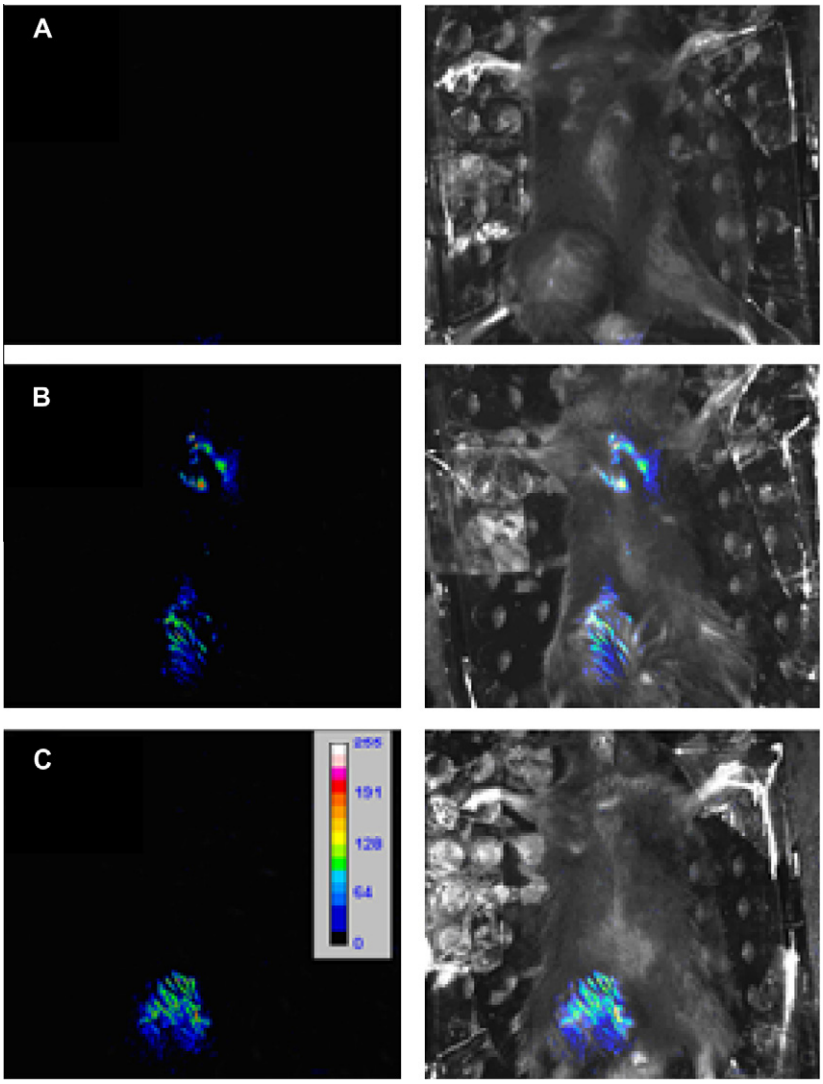


**Fig. 4.** Whole animal fluorescent image of mice after administration of (A) $QD_{576}$–POPC micelles, (B) QDs-*B. bifidum*, and (C) QDs-*B. bifidum*–FAs. Right column shows the fluorescence-merged images. The label bar depictured the fluorescent intensities.

improved by FAs modification of the bacteria surface. Combining the advantages of their intrinsic biocompatibility and the ease of preparation, the chemically modified *B. bifidum* could be used as a versatile vehicle to efficiently deliver probes and therapeutic reagents for cancer diagnostics and therapy.

## Acknowledgments

We appreciate Prof. Shigong Zheng, Peking University, and Mr. Bo Zhang, Beijing Cold Spring Co., for their help in animal experiments. This work is supported by NSFC (Project No. 20973008).

## Appendix A. Supplementary data

Supplementary data associated with this article can be found, in the online version, at http://dx.doi.org/10.1016/j.bbrc.2012.07.150.

## References

[1] B.O. Dabbousi, J. Rodriguez-Viejo, F.V. Mikulec, J.R. Heine, H. Mattoussi, R. Ober, K.F. Jensen, M.G. Bawendi, (CdSe)ZnS core–shell quantum dots: synthesis and characterization of a size series of highly luminescent nanocrystallites, J. Phys. Chem. B 101 (1997) 9463–9475.
[2] A.P. Alivisatos, Semiconductor clusters, nanocrystals, and quantum dots, Science 271 (1996) 933–937.
[3] S. Ravindran, S. Chaudhary, B. Colburn, M. Ozkan, C.S. Ozkan, Covalent coupling of quantum dots to multiwalled carbon nanotubes for electronic device applications, Nano Lett. 3 (2003) 447–453.
[4] W.W. Yu, E. Chang, R. Drezek, V.L. Colvin, Water-soluble quantum dots for biomedical applications, Biochem. Biophys. Res. Commun. 348 (2006) 781–786.
[5] Y.F. Loginova, S.V. Dezhurov, V.V. Zherdeva, N.I. Kazachkina, M.S. Wakstein, A.P. Savitsky, Biodistribution and stability of CdSe core quantum dots in mouse digestive tract following per os administration: advantages of double polymer/silica coated nanocrystals, Biochem. Biophys. Res. Commun. 419 (2012) 54–59.
[6] X. Michalet, F.F. Pinaud, L.A. Bentolila, J.M. Tsay, S. Doose, J.J. Li, G. Sundaresan, A.M. Wu, S.S. Gambhir, S. Weiss, Quantum dots for live cells, in vivo imaging, and diagnostics, Science 307 (2005) 538–544.
[7] I.L. Medintz, H.T. Uyeda, E.R. Goldman, H. Mattoussi, Quantum dot bioconjugates for imaging, labelling and sensing, Nat. Mater. 4 (2005) 435–446.
[8] H. Arya, Z. Kaul, R. Wadhwa, K. Taira, T. Hirano, S.C. Kaul, Quantum dots in bio-imaging: revolution by the small, Biochem. Biophys. Res. Commun. 329 (2005) 1173–1177.
[9] X.H. Gao, Y.Y. Cui, R.M. Levenson, L.W.K. Chung, S.M. Nie, In vivo cancer targeting and imaging with semiconductor quantum dots, Nat. Biotechnol. 22 (2004) 969–976.
[10] H. Tada, H. Higuchi, T.M. Wanatabe, N. Ohuchi, In vivo real-time tracking of single quantum dots conjugated with monoclonal anti-$HER_2$ antibody in tumors of mice, Cancer Res. 67 (2007) 1138–1144.
[11] W. Cai, D.-W. Shin, K. Chen, O. Gheysens, Q. Cao, S.X. Wang, S.S. Gambhir, X. Chen, Peptide-labeled near-infrared quantum dots for imaging tumor vasculature in living subjects, Nano Lett. 6 (2006) 669–676.
[12] B. Ballou, B.C. Lagerholm, L.A. Ernst, M.P. Bruchez, A.S. Waggoner, Noninvasive imaging of quantum dots in mice, Bioconjugate Chem. 15 (2004) 79–86.
[13] L. Chen, A.J. Zurita, P.U. Ardelt, R.J. Giordano, W. Arap, R. Pasqualini, Design and validation of a bifunctional ligand display system for receptor targeting, Chem. Biol. 11 (2004) 1081–1091.
[14] M.A. Dobrovolskaia, S.E. McNeil, Immunological properties of engineered nanomaterials, Nat. Nanotechnol. 2 (2007) 469–478.
[15] K.D. Arunachalam, Role of bifidobacteria in nutrition, medicine and technology, Nutr. Res. 19 (1999) 1559–1597.
[16] R.K. Jain, N.S. Forbes, Can engineered bacteria help control cancer? Proc. Natl. Acad. Sci. USA 98 (2001) 14748–14750.
[17] L.H. Dang, C. Bettegowda, D.L. Huso, K.W. Kinzler, B. Vogelstein, Combination bacteriolytic therapy for the treatment of experimental tumors, Proc. Natl. Acad. Sci. USA 98 (2001) 15155–15160.
[18] R.M. Ryan, J. Green, C.E. Lewis, Use of bacteria in anti-cancer therapies, Bioessays 28 (2006) 84–94.
[19] X. Li, G.F. Fu, Y.R. Fan, W.H. Liu, X.J. Liu, J.J. Wang, G.X. Xu, *Bifidobacterium adolescentis* as a delivery system of endostatin for cancer gene therapy: selective inhibitor of angiogenesis and hypoxic tumor growth, Cancer Gene Ther. 10 (2003) 105–111.
[20] K. Yazawa, M. Fujimori, J. Amano, Y. Kano, S. Taniguchi, *Bifidobacterium longum* as a delivery system for cancer gene therapy: selective localization and growth in hypoxic tumors, Cancer Gene Ther. 7 (2000) 269–274.
[21] N.T. Kimura, S. Taniguchi, T.B.K. Aoki, Selective localization and growth of *Bifidobacterium bifidum* in mouse-tumors following intravenous administration, Cancer Res. 40 (1980) 2061–2068.
[22] E. Jang, S. Jun, L. Pu, High quality CdSeS nanocrystals synthesized by facile single injection process and their electroluminescence, Chem. Commun. 24 (2003) 2964–2965.
[23] R. Han, M. Yu, Q. Zheng, L. Wang, Y. Hong, Y. Sha, A facile synthesis of small-sized, highly photoluminescent, and monodisperse CdSeS QD/$SiO_2$ for live cell imaging, Langmuir 25 (2009) 12250–12255.
[24] M. Yu, Y. Yang, R. Han, Q. Zheng, L. Wang, Y. Hong, Z. Li, Y. Sha, Polyvalent lactose-quantum dot conjugate for fluorescent labeling of live leukocytes, Langmuir 26 (2010) 8534–8539.
[25] D.J.A. Crommelin, M. Grit, H. Talsma, N.J. Zuidam, Liposomes as carriers for drugs and antigens: approaches to preserve their long term stability, Drug Dev. Ind. Pharm. 20 (1994) 547–556.
[26] S.K. Hobbs, W.L. Monsky, F. Yuan, W.G. Roberts, L. Griffith, V.P. Torchilin, R.K. Jain, Regulation of transport pathways in tumor vessels: role of tumor type and microenvironment, Proc. Natl. Acad. Sci. USA 95 (1998) 4607–4612.
27 P.W. Vaupel, Oxygenation of solid tumors, in: B.A. Teicher (Ed.), Drug Resistance in Oncology, Marcel Dekker, New York, 1993, pp. 53–85.
[28] M.T. Peracchia, E. Fattal, D. Desmaele, M. Besnard, J.P. Noel, J.M. Gomis, M. Appel, J. d'Angelo, P. Couvreur, Stealth (R) PEGylated polycyanoacrylate nanoparticles for intravenous administration and splenic targeting, J. Control. Release 60 (1999) 121–128.
[29] O. Trédan, C.M. Galmarini, K. Patel, I.F. Tannock, Drug resistance and the solid tumor microenvironment, J. Natl. Cancer Inst. 99 (2007) 1441–1454.
[30] A.I. Minchinton, I.F. Tannock, Drug penetration in solid tumours, Nat. Rev. Cancer 6 (2006) 583–592.